Atomistic Spin-Lattice Dynamics

47

Pui-Wai Ma and S. L. Dudarev

Contents

Abstract

Finite temperature magnetic fluctuations determine a variety of properties of magnetic materials, including their phase stability, their thermodynamic properties, and even the structure of defects formed under irradiation. A fundamental feature of microscopic magnetic fluctuations is the directional non-collinearity of fluctuating atomic magnetic moments, which stems from the rotational invariance of an atomic magnetic Hamiltonian. To model the dynamics of magnetic moments of atoms that move themselves, a fast and computationally efficient simulation approach is required. Spin-lattice dynamics simulates atomic movements as well as rotational and longitudinal fluctuations of atomic magnetic moments within a unified framework, generalizing molecular dynamics

P.-W. Ma (✉) · S. L. Dudarev
Culham Centre for Fusion Energy, UK Atomic Energy Authority, Culham Science Centre, Abingdon, UK
e-mail: Leo.Ma@ukaea.uk

W. Andreoni, S. Yip (eds.), *Handbook of Materials Modeling*,
https://doi.org/10.1007/978-3-319-44677-6_97

to magnetic materials. Collective magnetic and atomic excitations can now be investigated on the microscopic scale, similarly to how transformations of atomic structures can be investigated using molecular dynamics simulations. This chapter outlines theoretical foundations and numerical algorithms of spin-lattice dynamics and describes applications of the method.

1 Introduction

Magnetic materials play a pivotal part in modern technology; their applications include long-term information storage, fast access memory devices, and even quantum computing. Magnetic and mechanical properties of magnetic materials are intimately related, in particular this applies to steels and iron alloys. For example, ferromagnetic iron is the only element in Group 8 of the Periodic Table that adopts the bcc crystal structure. All the other elements in the same group have hcp crystal structure, and bcc Fe owes its stability to magnetism (Pettifor 1995). A self-interstitial atom defect in bcc iron adopts a ⟨110⟩ dumbbell configuration (Fu et al. 2004), whereas in all the nonmagnetic bcc metals, a single self-interstitial defect has the ⟨111⟩ symmetry (Nguyen-Manh et al. 2006; Derlet et al. 2007). At high temperatures, bcc-fcc-bcc phase transitions in iron occur as a result of competition between magnetic excitations and atomic vibrations (Lavrentiev et al. 2010; Ma et al. 2017).

Neither molecular dynamics nor spin dynamics on their own can capture *both* magnetic and atomic excitations. A broader mathematical simulation framework is required to describe the dynamics of spin and lattice subsystems and their coupling. Omelyan et al. (2001a,b, 2002) and Tsai et al. (2004, 2005) proposed models unifying spin dynamics and molecular dynamics. We have developed their ideas further, arriving at an algorithm suitable for simulating real materials.

Spin-lattice dynamics follows the time evolution of coupled spin and lattice subsystems. Precession of spins and atomic motion are coupled through spin-dependent forces and coordinate-dependent effective exchange fields. Figure 1 shows snapshots of magnetic order in iron at 0 and 300 K. The figure illustrates an important aspect of finite temperature magnetic simulations. Magnetic moments (which sometimes are also called atomic spins) become non-collinear due to thermal excitation. The fact that interaction between magnetic moments depends on the position of atoms, generates additional, spin direction dependent, forces acting between the atoms in the material. This is how magnetic excitations affect the dynamics and stability of atomic lattice.

In what follows, we first discuss the spin equations of motion and the notion of spin temperature. Then, we outline theoretical foundations of spin-lattice dynamics. We also describe a numerical integration algorithm that does not normally receive much attention in the context of molecular dynamics but proves essential in the framework of spin-lattice dynamics. Finally, we highlight the still outstanding scientific challenges, particularly those associated with magnetic many-body interatomic interaction potentials.

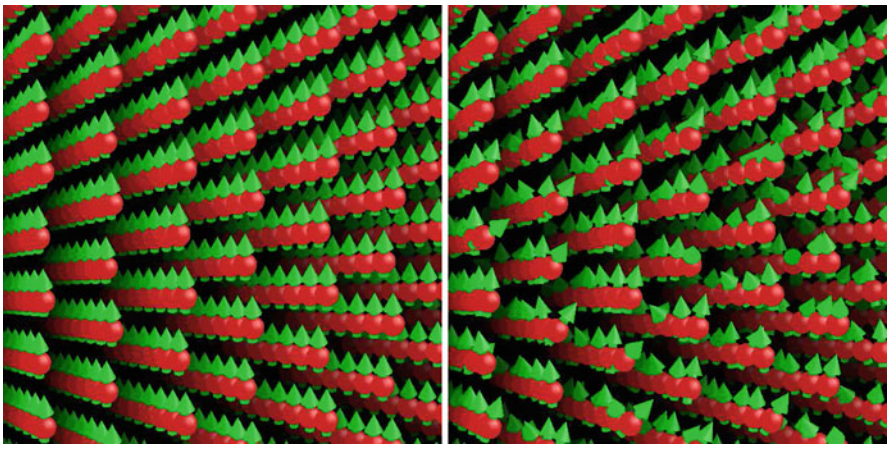

Fig. 1 Snapshots of magnetic configurations generated using spin-lattice dynamics simulations of iron at 0 and 300 K. Simulations were performed using spin-lattice dynamics simulation program SPILADY (Ma et al. 2016)

2 The Quantum Origin of Spin Dynamics

The localized nature of d and f electrons justifies the notion of an atomic magnetic moment $\mathbf{M}$ or atomic spin $\mathbf{S}$, where $\mathbf{M} = -g\mu_B\mathbf{S}$, g is the electron g-factor, and μ_B is the Bohr magneton. Atomic magnetic moments form due to intra-atomic exchange interaction between the localized electrons. Interaction between magnetic moments associated with different atoms can be understood as resulting from the interplay between intra-atomic exchange and interatomic quantum hopping of electrons. The quantum nature of atomic spins gives rise to their unusual properties, for example, an atomic spin has no mass and hence has no conjugate variable. The classical equation of motion for a spin vector is in fact the mean-field analog of the quantum equation of motion for the spin operator, which can be derived using the Poisson brackets approach (Ma and Dudarev 2012).

Consider an arbitrary quantum-mechanical spin Hamiltonian $\hat{\mathscr{H}}$. It can be expressed as a Taylor series in the spin vector operator $\hat{\mathbf{S}}$ as

$$\hat{\mathscr{H}} = \sum_{n=0}^{\infty} \mathbf{a}_n \hat{\mathbf{S}}^n, \tag{1}$$

where tensor quantities $\mathbf{a}_n$ are the Taylor series expansion coefficients. The n^{th} order of operator $\hat{\mathbf{S}}$ can be written as

$$\begin{aligned} \hat{\mathbf{S}}^n &= (\hat{\mathbf{I}}\mathbf{S} + \delta\hat{\mathbf{S}})^n, \\ &= \hat{\mathbf{I}}\mathbf{S}^n + n\mathbf{S}^{n-1}\delta\hat{\mathbf{S}} + \cdots, \end{aligned} \tag{2}$$

where $\mathbf{S}$ is the expectation value of $\hat{\mathbf{S}}$, $\hat{\mathbf{I}}$ is the identity operator, and $\delta\hat{\mathbf{S}} = \hat{\mathbf{S}} - \hat{\mathbf{I}}\mathbf{S}$ is what can be called the deviation of the operator from its expectation value. Substituting Eq. (2) into Eq. (1), we find

$$\begin{aligned}\hat{\mathscr{H}} &= \hat{\mathbf{I}}\sum_{n=0}^{\infty}\mathbf{a}_n\mathbf{S}^n + \sum_{n=1}^{\infty}\mathbf{a}_n n\mathbf{S}^{n-1}\delta\hat{\mathbf{S}} + \cdots, \\ &= \hat{\mathbf{I}}\mathscr{H} + \frac{\partial\mathscr{H}}{\partial\mathbf{S}}\cdot\delta\hat{\mathbf{S}} + \cdots. \end{aligned} \tag{3}$$

The first term in (3) is the Hamiltonian *function* $\mathscr{H}$, which is equivalent to a classical Hamiltonian, where the spin operator $\hat{\mathbf{S}}$ is replaced by its expectation value $\mathbf{S}$. Ignoring higher-order terms in Eq. (3), the equation of motion for a spin operator can be derived using the Poisson brackets commutator

$$\begin{aligned}\frac{d\hat{\mathbf{S}}}{dt} &= \frac{i}{\hbar}\left[\hat{\mathscr{H}}, \hat{\mathbf{S}}\right] = \frac{1}{\hbar}\left[\hat{\mathbf{S}}\times\left(-\frac{\partial\mathscr{H}}{\partial\mathbf{S}}\right)\right], \\ &= \frac{1}{\hbar}\left[\hat{\mathbf{S}}\times\mathbf{H}\right], \end{aligned} \tag{4}$$

where $\mathbf{H} = -\partial\mathscr{H}/\partial\mathbf{S}$ is the effective field acting on spin $\hat{\mathbf{S}}$. Since the first term in Eq. (3) commutes with $\hat{\mathbf{S}}$, it gives no contribution to the equation of motion. The first non-vanishing contribution to the right-hand side of (4) comes from the second term in Eq. (3).

The above derivation remains valid for any spin Hamiltonian. We note that the form of Eq. (4) is the same as that of the equation of motion for a classical spin vector. This can be proven by evaluating expectation values of both sides of the equation.

3 Spin Temperature Monitoring and Control

If a statistical and dynamically evolving system is in contact with another statistical, and also dynamically evolving, system, energy flows from the hotter to the cooler one, until they reach thermal equilibrium. There is an established procedure for thermalizing an atomic system in a molecular dynamics simulation, which involves putting the system in contact with a heat reservoir, represented by certain fluctuation and dissipation terms in the classical equations of motion for the atoms. This thermalization method is known as Langevin dynamics. The treatment of Brownian motion is probably one of the best known examples of application of the method (Chandrasekhar 1943; Kubo 1966). The use of Langevin dynamics for equilibrating and thermalizing large systems of interacting atoms is a well-established part of the molecular dynamics simulation toolkit.

In the preceding section, we derived equations of motion for a closed system of interacting spins. To thermalize a spin system, one can also use a special form of Langevin dynamics, the implementation of which requires suitably modified spin equations of motion. Langevin dynamics approach to spin dynamics was proposed by Brown (1963). For an arbitrary Hamiltonian $\mathscr{H}(\{\mathbf{S}_i\})$ describing N atomic spins, the Langevin equation of motion for an atomic spin vector i can be written as

$$\frac{d\mathbf{S}_i}{dt} = \frac{1}{\hbar}\left[\mathbf{S}_i \times (\mathbf{H}_i + \mathbf{h}_i) - \gamma \mathbf{S}_i \times (\mathbf{S}_i \times \mathbf{H}_i)\right] \tag{5}$$

where $\mathbf{H}_i = -\partial\mathscr{H}/\partial\mathbf{S}_i$ is the effective magnetic field acting on atomic spin i, γ is a dissipation constant, and $\mathbf{h}_i$ is a delta-correlated fluctuating vector satisfying conditions $\langle \mathbf{h}_i(t)\rangle = 0$ and $\langle h_{i\alpha}(t) h_{j\beta}(t')\rangle = \mu\delta_{ij}\delta_{\alpha\beta}\delta(t-t')$. Subscripts α and β refer to the Cartesian components of a vector, and parameter μ characterizes the magnitude of thermal magnetic fluctuations.

Stochastic and dissipative forces acting together drive a dynamic system to thermal equilibrium. Fluctuation and dissipation terms are related through the fluctuation-dissipation theorem (Chandrasekhar 1943; Kubo 1966). The fluctuation-dissipation relation (FDR) between the fluctuating and dissipative terms can be obtained by mapping the Langevin equation of motion to a Fokker-Planck equation (Zwanzig 2001; Van Kampen 2011) and identifying the asymptotic stationary solution of that equation with the Gibbs distribution (Brown 1963; Ma and Dudarev 2011). The FDR for Eq. (5) reads $\mu = 2\gamma\hbar k_B T$, where T is the temperature of the heat reservoir. Without the fluctuating term, Eq. (5) reduces to the Landau-Lifshitz equation (Landau and Lifshitz 1935; Gilbert 2004), which contains only the dissipative term. In the asymptotic limit $t \to \infty$, solutions of the Landau-Lifshitz equation describe stationary spin configurations, where $d\mathbf{S}_i/dt = 0$. Directions of vectors $\mathbf{S}_i$ in a stationary spin configuration can be found by solving equations $\mathbf{S}_i \times \mathbf{H}_i = 0$, where $i = 1, 2 \ldots N$ (see Lavrentiev et al. 2011). The latter condition has a simple meaning, namely, that in the lowest energy configuration every spin vector $\mathbf{S}_i$ is collinear with the exchange field $\mathbf{H}_i$ acting on it.

A notable feature of Eq. (5) is that the magnitude of the spin vector $|\mathbf{S}_i(t)|$, where $\mathbf{S}_i(t)$ is a solution of the equation, remains constant. This can be easily proven by multiplying both sides of the equation by $\mathbf{S}_i$ and noting that a vector product, involving an arbitrary vector, is orthogonal to it. As a result, the magnitude of the spin vector is conserved $d\mathbf{S}_i^2(t)/dt = 0$.

Due to the simultaneously localized and itinerant nature of electrons in a solid, both the magnitude and direction of atomic spins are variable quantities. A revision of Langevin spin dynamics is required to relax the constraint that the magnitude of an evolving spin vector is a constant. Bearing in mind the Langevin treatment of atomic dynamics, we find that longitudinal fluctuations of an atomic magnetic moment, i.e., fluctuations of the magnitude of a spin vector, can indeed be treated using some suitably chosen fluctuation and dissipation terms (Ma and Dudarev 2012). We write

$$\frac{d\mathbf{S}_i}{dt} = \frac{1}{\hbar}\left[\mathbf{S}_i \times \left(-\frac{\partial \mathscr{H}}{\partial \mathbf{S}_i}\right)\right] - \gamma \frac{\partial \mathscr{H}}{\partial \mathbf{S}_i} + \boldsymbol{\xi}_i, \tag{6}$$

$$= \frac{1}{\hbar}\left[\mathbf{S}_i \times \mathbf{H}_i\right] + \gamma \mathbf{H}_i + \boldsymbol{\xi}_i, \tag{7}$$

where $\boldsymbol{\xi}_i$ is a delta-correlated fluctuating vector satisfying conditions $\langle \boldsymbol{\xi}_i(t) \rangle = 0$ and $\langle \xi_{i\alpha}(t)\xi_{j\beta}(t') \rangle = \mu \delta_{ij}\delta_{\alpha\beta}\delta(t-t')$. The FDR can now be obtained by mapping Eq. (6) onto a Fokker-Planck equation (Zwanzig 2001; Van Kampen 2011):

$$\frac{\partial W}{\partial t} = -\sum_{i\alpha} \frac{\partial}{\partial S_{i\alpha}}(A_{i\alpha} W) + \frac{1}{2}\sum_{ij\alpha\beta} \frac{\partial^2}{\partial S_{i\alpha}\partial S_{j\beta}}(B_{i\alpha j\beta} W). \tag{8}$$

In the above equation, $A_{i\alpha} = \lim_{\Delta t \to 0} \frac{1}{\Delta t}\langle S_{i\alpha} \rangle$ is an effective drift coefficient, and $B_{i\alpha j\beta} = \lim_{\Delta t \to 0} \frac{1}{\Delta t}\langle S_{i\alpha} S_{j\beta} \rangle$ is an effective diffusion coefficient. According to Eq. (6), the drift and diffusion coefficients have the form (Zwanzig 2001; Van Kampen 2011):

$$\mathbf{A}_i = \frac{1}{\hbar}\left[\mathbf{S}_i \times \left(-\frac{\partial \mathscr{H}}{\partial \mathbf{S}_i}\right)\right] - \gamma \frac{\partial \mathscr{H}}{\partial \mathbf{S}_i}, \tag{9}$$

$$B_{i\alpha j\beta} = \mu \delta_{ij}\delta_{\alpha\beta}. \tag{10}$$

In thermal equilibrium, the energy distribution asymptotically approaches the Gibbs distribution $W = W_0 \exp(-\mathscr{H}/k_B T)$, where W_0 is a normalization constant. Substituting Eqs. (9) and (10), and the Gibbs distribution, into Eq. (8), one finds that

$$\frac{\partial W}{\partial t} = \left(\gamma - \frac{\mu}{2k_B T}\right)\left[\sum_{i,\alpha}\left(\frac{\partial^2 \mathscr{H}}{\partial S_{i\alpha}^2} - \frac{1}{k_B T}\left(\frac{\partial \mathscr{H}}{\partial S_{i\alpha}}\right)^2\right)\right] W. \tag{11}$$

Stationary solutions of this equation corresponding to $\partial W/\partial t = 0$ describe thermal equilibrium. From Eq. (11) we see that the right-hand side of Eq. (11) vanishes if

$$\mu = 2\gamma k_B T. \tag{12}$$

Surprisingly, the form of this FDR is exactly the same as that of the lattice Langevin dynamics. The right-hand side of Eq. (11) also vanishes if

$$k_B T = \sum_{i,\alpha}\left(\frac{\partial \mathscr{H}}{\partial S_{i\alpha}}\right)^2 \Bigg/ \sum_{i,\alpha} \frac{\partial^2 \mathscr{H}}{\partial S_{i\alpha}^2}. \tag{13}$$

Equation (13) defines the dynamic spin temperature at equilibrium as a function of microscopic dynamic variables. This resembles the well-known equipartition principle for atoms where the lattice temperature can be estimated using the relation $3Nk_B T/2 = \sum_i \mathbf{P}_i^2/2m$, where $\mathbf{P}_i$ is the momentum of atom i. Equation (13)

has similar functionality, and it can also be used for estimating the local spin temperature of an arbitrary spin configuration, which potentially may be very far from equilibrium. Applying a similar procedure to Eq. (5), we find an alternative formula for the spin temperature, which applies if the longitudinal fluctuations of magnetic moments can be neglected (Ma et al. 2010).

$$k_B T = \frac{\sum_i |\mathbf{S}_i \times \mathbf{H}_i|^2}{2 \sum_i \mathbf{S}_i \cdot \mathbf{H}_i}. \tag{14}$$

Here we note an alternative way of deriving Eqs. (13) and (14). If a system is in thermal equilibrium, there is no net energy exchange with the heat reservoir, resulting in $d\langle E \rangle / dt = 0$. Since $dE/dt = \sum_i (\partial E / \partial \mathbf{S}_i)(d\mathbf{S}_i/dt)$, by using either of the two forms of Langevin equations of motion for the spins, taking the ensemble average, and applying the FDR, we arrive at the above formulae for the spin temperature expressed in terms of dynamic spin variables. Condition $T = 0$ corresponds to the lowest energy spin configuration that, according to Eq. (14), is defined by a set of algebraic equations noted earlier in this section, namely, $\mathbf{S}_i \times \mathbf{H}_i = 0$ for $i = 1, 2 \ldots, N$.

4 Spin-Lattice Dynamics

Interaction between atoms in a magnetic material is determined by its spin-dependent electronic structure. A suitable mathematical framework is required to describe the many-body phonon and magnon excitations at elevated temperature. Conventional molecular dynamics provides a convenient starting point for the incorporation of spin degrees of freedom in an atomistic simulation. It is possible to reformulate molecular dynamics and spin dynamics and combine them within a unified simulation framework. This also makes it possible to treat interaction between the lattice and magnetic subsystems, where interatomic forces and effective exchange fields acting on magnetic moments are related and dynamically coupled with each other.

Consider an arbitrary coordinate and spin-dependent Hamiltonian $\mathscr{H}(\mathbf{R}, \mathbf{P}, \mathbf{S})$, where $\mathbf{R} = \{\mathbf{R}_i\}$ are the atomic coordinates, $\mathbf{P} = \{\mathbf{P}_i\}$ are the atomic momenta, and $\mathbf{S} = \{\mathbf{S}_i\}$ are the atomic spin vectors. The Hamilton equations of motion for a closed system have the form (Ma et al. 2008, 2016):

$$\begin{aligned} \frac{d\mathbf{R}_i}{dt} &= \frac{\partial \mathscr{H}}{\partial \mathbf{P}_i}, \\ \frac{d\mathbf{P}_i}{dt} &= -\frac{\partial \mathscr{H}}{\partial \mathbf{R}_i}, \\ \frac{d\mathbf{S}_i}{dt} &= \frac{1}{\hbar}\left[\mathbf{S}_i \times \left(-\frac{\partial \mathscr{H}}{\partial \mathbf{S}_i}\right)\right]. \end{aligned} \tag{15}$$

From their appearance, these equations formally amount to no more than a combination of molecular dynamics and spin dynamics, and the only quantity that formally unifies them is the Hamiltonian. However, there is a subtle difference between spin-lattice dynamics defined by Eqs. (15) above and molecular dynamics or spin dynamics treated as separate simulation methods. The force $\mathbf{F}_i = -\partial\mathscr{H}/\partial\mathbf{R}_i$ acting on atom i and the effective magnetic field $\mathbf{H}_i = -\partial\mathscr{H}/\partial\mathbf{S}_i$ acting on spin vector i are coordinate *and* spin-dependent. The direction and magnitude of atomic spin vectors $\mathbf{S}_i$ affect the direction and magnitude of forces acting between the atoms in a magnetic material, whereas the effective exchange field acting on spin $\mathbf{S}_i$ depends on atomic positions. The lattice and spin subsystems are now coupled through the spin-orientation-dependent interatomic forces and coordinate-dependent effective exchange fields.

Generalizing Eqs. (15) to Langevin dynamics, we write the Langevin equations of motion for the spins and atomic coordinates and momenta as

$$\begin{aligned}
\frac{d\mathbf{R}_i}{dt} &= \frac{\partial\mathscr{H}}{\partial\mathbf{P}_i},\\
\frac{d\mathbf{P}_i}{dt} &= -\frac{\partial\mathscr{H}}{\partial\mathbf{R}_i} - \gamma_l\frac{\partial\mathscr{H}}{\partial\mathbf{P}_i} + \mathbf{f}_i,\\
\frac{d\mathbf{S}_i}{dt} &= \frac{1}{\hbar}\left[\mathbf{S}_i \times \left(-\frac{\partial\mathscr{H}}{\partial\mathbf{S}_i}\right)\right] - \gamma_s\frac{\partial\mathscr{H}}{\partial\mathbf{S}_i} + \boldsymbol{\xi}_i,
\end{aligned} \tag{16}$$

where $\mathbf{f}_i$ and $\boldsymbol{\xi}_i$ are the fluctuating components of interatomic forces and exchange fields, respectively. They satisfy the Langevin equations conditions $\langle\mathbf{f}_i(t)\rangle = 0$ and $\langle f_{i\alpha}(t)f_{j\beta}(t')\rangle = \mu_l\delta_{ij}\delta_{\alpha\beta}\delta(t-t')$ for the fluctuating components of interatomic forces and $\langle\boldsymbol{\xi}_i(t)\rangle = 0$ and $\langle\xi_{i\alpha}(t)\xi_{j\beta}(t')\rangle = \mu_s\delta_{ij}\delta_{\alpha\beta}\delta(t-t')$ for the fluctuating exchange fields. The FDR relations for the lattice and spin subsystems read $\mu_l = 2\gamma_l k_B T$ and $\mu_s = 2\gamma_s k_B T$, where T is the temperature of the heat reservoir. The dissipative constants γ_l and γ_s determine the thermalization rates, which can be derived from experimental observations. An example of thermalization process is given in Fig. 2. The figure shows how the spin and lattice temperatures vary in an interacting spin-lattice dynamic system. The simulation involves 16,000 magnetic atoms of iron. The reservoir temperature is set to 300 K. We used the values of parameters describing ferromagnetic iron that were derived by Ma and Dudarev (2012) and Ma et al. (2012). The different thermalization rates characterizing spin and lattice subsystems are primarily due to the difference between the values of dissipation constants γ_l and γ_s.

The spin-lattice dynamics simulation model can be extended to include the treatment of conduction electrons, if we assume that there is a significant amount of heat dissipated to the electrons. This is often the case in metals. For example, in applications, the heat reservoir is nothing but the time-dependent evolving electron subsystem. Its dynamic behavior is described by the heat transfer equation

$$C_e\frac{dT_e}{dt} = \nabla(\kappa_e\nabla T_e) + G_{el}(T_l - T_e) + G_{es}(T_s - T_e), \tag{17}$$

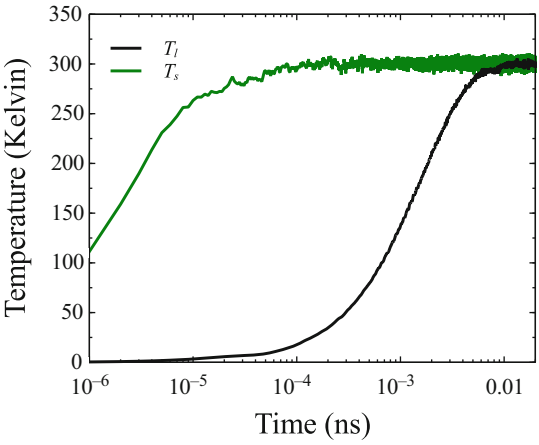

Fig. 2 Spin and lattice temperatures in magnetic iron during thermalization, predicted by spin-lattice dynamics simulations. The temperature of the reservoir is 300 K. Initial temperatures of atoms and spins are $T = 0$ K. The simulation follows the evolution of 16,000 magnetic iron atoms, initially forming a perfect bcc lattice configuration

where C_e is the electronic specific heat and κ_e is the coefficient of thermal conductivity. The coupling constants describing interaction between electron and lattice subsystems G_{el} and between electron and spin subsystems G_{es} are

$$G_{el} = \frac{3k_B\gamma_l}{m\Omega} \tag{18}$$

$$G_{es} = \frac{k_B\gamma_s}{\Omega}\langle\sum_{\alpha}\frac{\partial^2\mathscr{H}}{\partial S_{i\alpha}^2}\rangle \tag{19}$$

where Ω is the atomic volume. Detailed derivations of G_{el} and G_{es} are given in Ma et al. (2012, 2016) and references therein. Equations (16) and (17) constitute a fully self-consistent atomistic spin-lattice-electron model. In the ultrafast laser experiments, where over a relatively short period of time only a small amount of heat is exchanged with the environment, the spin-lattice-electron model can be successfully applied to modelling transient processes of thermalization and heat exchange between the three subsystems, as well as to the treatment of fast demagnetization (Ma et al. 2016).

5 The Suzuki-Trotter Decomposition

In a dynamic simulation of the evolution of a system of atoms, a numerical algorithm advances the state of the system as a function of time by propagating a configuration through a sequence of finite time steps. This generates numerical errors, for example, biased errors and truncation errors, resulting from analytical or numerical approximations. An integration algorithm based on the Suzuki-Trotter decomposition (STD) (Hatano and Suzuki 2005) can minimize numerical errors over a relatively long interval of computation time due to its symplectic nature,

which means that the algorithm conserves the phase space volume of the system during evolution. The STD involves breaking up an evolution operator, which consists of several noncommutative operations, into simpler sub-evolution steps. The second-order STD has the form

$$e^{(\hat{A}+\hat{B})\Delta t} = e^{\hat{A}\Delta t/2} e^{\hat{B}\Delta t} e^{\hat{A}\Delta t/2} + O(\Delta t^3) \tag{20}$$

where $\hat{A}$ and $\hat{B}$ are arbitrary operators and Δt is the time step. The above formula describes how to decompose an operator that evolves the system over a time step, into several simpler evolution steps, each involving the evolution of only a subset of variables describing the microscopic configuration of the system.

Omelyan et al. (2001a,b, 2002) and Tsai et al. (2004, 2005) explored applications of the STD to spin-lattice dynamics, and in what follows we adopt a similar approach. Equations of motion for a spin-lattice system can be rewritten as

$$\frac{d\mathbf{x}}{dt} = (\mathscr{R} + \mathscr{P} + \mathscr{S})\mathbf{x}, \tag{21}$$

where $\mathbf{x} = \{\mathbf{R}, \mathbf{P}, \mathbf{S}\}$ is a generalized coordinate and $\mathscr{R}$, $\mathscr{P}$, $\mathscr{S}$ are the evolution operators acting on $\mathbf{R}$, $\mathbf{P}$, and $\mathbf{S}$, respectively. The formal solution of Eq. (21) can be written as

$$\mathbf{x}(t + \Delta t) = e^{(\mathscr{R}+\mathscr{P}+\mathscr{S})\Delta t}\mathbf{x}(t). \tag{22}$$

Using the STD decomposition given by Eq. (20), we write

$$e^{(\mathscr{R}+\mathscr{P}+\mathscr{S})\Delta t} = e^{\mathscr{P}\Delta t/2} e^{\mathscr{S}\Delta t/2} e^{\mathscr{R}\Delta t} e^{\mathscr{S}\Delta t/2} e^{\mathscr{P}\Delta t/2} + O(\Delta t^3). \tag{23}$$

Reading the right-hand side of this equation from right to left, we see that the STD decomposition rule requires that we would integrate equations for the momenta of particles over the time interval $\Delta t/2$, then integrate equations for the spins over the time interval $\Delta t/2$, and then integrate equations for atomic coordinates over the time interval Δt, followed by the integration of equations for the spins over $\Delta t/2$ and equations for the momenta over $\Delta t/2$. The order in which we integrate the equations minimizes the number of times where forces are evaluated and significantly reduces the time required to do a simulation. The main advantage offered by the STD (23) is that it circumvents the need to integrate the coupled equations for the coordinates, momenta, and spins all at the same time.

A particular subtlety associated with the presence of spin equations of motion in Eqs. (15) is that spin dynamics involve rotations, which, as opposed to translations, do not commute. Bearing this in mind, the evolution of the spin subsystem can be split into a series of operations involving evolution of individual spins, namely

$$e^{\mathscr{S}\Delta t} = e^{\mathscr{S}_1\Delta t/2} e^{\mathscr{S}_2\Delta t/2} \cdots e^{\mathscr{S}_N\Delta t} \cdots e^{\mathscr{S}_2\Delta t/2} e^{\mathscr{S}_1\Delta t/2} + O(\Delta t^3). \tag{24}$$

Each operation of evolution of an individual spin depends on all the previous operations, because the effective magnetic field $\mathbf{H}_i$ acting on spin i depends on the entire configuration $\mathbf{S}$ of all the other spins. In serial programming, one only needs to integrate the equations of motion for individual spins in a certain order, determined by the STD decomposition (24), one equation at a time. However, Eq. (24) prohibits performing multiple spin operations at the same time, in effect prohibiting the parallelization of the integration algorithm.

Parallel integration of spin equations of motion is still possible if interaction between the spins has a finite spatial extent (Ma and Woo 2009). In this case the effective exchange field acting on a spin depends only on a finite number of neighboring spins. The simulation cell can then be subdivided into separate spatial regions, where spins belonging to different regions do not interact. Spins can then be separated into noninteracting groups, and the STD can then be applied to the groups. The integration algorithm can then be parallelized between the groups, rather than between individual spins. An intrinsic part of an MD simulation program is the linked cells algorithm. A linked cell is a local spatial region, ideally suited for the parallel implementation of the STD of evolving spin operators. The parallel implementation of spin-lattice dynamics, adopted here, relies on and benefits from the linked cells decomposition of the simulation cell (Ma and Woo 2009).

6 Interatomic Potentials

In the sections above, we derived equations of motion and integration algorithms for spin-lattice dynamics simulations. These simulation algorithms have now been implemented in the form of a computer program SPILADY (Ma et al. 2016). The outstanding scientific challenge in spin-lattice dynamics is the development of high-fidelity interatomic potentials, suitable for modelling the microscopic dynamics of atoms and spins in magnetic materials, composed of various chemical elements. Similarly to the interatomic potentials used in molecular dynamics (Finnis 2003), an interatomic potential can have any functional form and can be parameterized in an arbitrary way, provided that it describes the physical properties that are of interest to applications. In most cases, potentials are fitted to data derived from ab initio calculations as well as to the data derived from experimental observations. There is no universal potential yet available for any material that would be able to predict energies and forces acting between the atoms in an arbitrary atomic configuration in good agreement with ab initio calculations.

In our work, we have adopted a relatively simple functional form of the many-body non-collinear spin-lattice potential. The potential can be derived from the Hamiltonian of the form

$$\mathscr{H} = \sum_i \frac{\mathbf{P}_i^2}{2m} + U(\mathbf{R}, \mathbf{S}). \tag{25}$$

In the above Hamiltonian, the potential energy U of a system with N magnetic atoms is written as a function of atomic coordinates and spin vectors. One can write the energy in a Taylor series in spin variables $\mathbf{S}$. Retaining only the rotationally invariant terms, we write (Dudarev and Derlet 2007)

$$U(\mathbf{R},\mathbf{S}) = U^{(0)}(\mathbf{R}) + \sum_i U_i^{(1)}(\mathbf{R})\mathbf{S}_i^2 + \sum_{ij} U_{ij}^{(2)}(\mathbf{R})\mathbf{S}_i\cdot\mathbf{S}_j + \sum_i U_i^{(3)}(\mathbf{R})\mathbf{S}_i^4 + \cdots . \tag{26}$$

This makes it possible to map Eq. (25) to a nonmagnetic many-body interatomic potential complemented with a Heisenberg-Landau Hamiltonian

$$U = U_l(\mathbf{R}) - \frac{1}{2}\sum_{ij} J_{ij}(\mathbf{R})\mathbf{S}_i\cdot\mathbf{S}_j + \sum_i A_i(\mathbf{R})\mathbf{S}_i^2 + \sum_i B_i(\mathbf{R})\mathbf{S}_i^4, \tag{27}$$

where $J_{ij}(\mathbf{R})$ is a coordinate-dependent exchange coupling function and $A_i(\mathbf{R})$ and $B_i(\mathbf{R})$ are the coordinate-dependent Landau coefficients. For the nonmagnetic "lattice" part $U_l(\mathbf{R})$ of the potential, we have adopted the embedded atom method (EAM) (Daw and Baskes 1984) functional form and assumed that the Landau coefficients A_i and B_i are functions of the effective electron density. This is by no means the only way of representing the non-collinear spin-lattice potential. However, this particular functional form has at least two advantages. Firstly, it has a clear physical meaning. The Heisenberg term describes spin-spin interactions, whereas the Landau terms describe longitudinal fluctuations of $\mathbf{S}_i$. Exchange coupling and the Landau coefficients depend on atomic coordinates, which couple the spin and lattice subsystems through forces and effective magnetic fields. Secondly, the spin and lattice equations of motion have a relatively simple form, which assists the numerical implementation of the algorithm.

A remarkable property of Eq. (27) is that in the nonmagnetic limit $\mathbf{S} = \mathbf{0}$, the spin-lattice interaction potential reduces to a conventional molecular dynamics many-body potential. This poses a question about the type of data required for fitting a spin-lattice interatomic interaction potential. The above argument shows that data on magnetic as well as on nonmagnetic atomic configurations are required, as in potential (27) one can switch on and off the magnetic spin-dependent part. Experimental observations do not always provide information about magnetic and nonmagnetic properties at the same time, making ab initio calculations an invaluable and irreplaceable source of data required for fitting spin-dependent potentials. Also, ab initio calculations allow greater freedom for preconditioning, for example, through the exploration of many non-collinear magnetic configurations in a variety of atomic environments.

The functional form of the potential given by Eq. (27) does not take into account spin-orbit coupling. Spin-orbit coupling allows the transfer of angular momentum and energy from the spin to the lattice subsystem and vice versa. Perera et al. (2016) proposed a phenomenological model for the magneto-crystalline anisotropy, which models the effect of spin-orbit coupling. They add an anisotropic term to the Hamiltonian

$$\mathscr{H}_{\text{aniso}} = -C_1 \sum_i \mathbf{K}_i \cdot \mathbf{S}_i - C_2 \sum_i \mathbf{S}_i^T \cdot \boldsymbol{\Lambda}_i \cdot \mathbf{S}_i, \tag{28}$$

where C_1 and C_2 are adjustable parameters. $\mathbf{K}_i(\mathbf{R}) = \partial \rho_i(\mathbf{R})/\partial \mathbf{R}_i$ and $\Lambda_{i,\alpha\beta}(\mathbf{R}) = \partial^2 \rho_i(\mathbf{R})/\partial R_{i\alpha} \partial R_{i\beta}$ are the coordinate-dependent functions defining the character of the on-site magnetic anisotropy, where $\rho_i(\mathbf{R})$ describes the symmetry of local environment. This approach may help treat the effect of magneto-crystalline anisotropy, although the link between (28) and the microscopic quantum-mechanical spin-orbit coupling Hamiltonian requires further analysis.

In the study of bcc-fcc-bcc phase transitions in pure iron (Ma et al. 2017), we have fitted a new spin-lattice potential using ab initio data as input. The functional form of the spin-dependent potential was assumed to be given by Eq. (27). In the process of fitting the potential, we have generated large data sets using ab initio calculations. The data included bcc, fcc, bct, rhombohedral, amorphous, and various defect structures under the constraint that the system remained entirely nonmagnetic. Using the data, we have fitted an EAM potential, which is the first term in (27). Then, we fitted the magnetic terms, separately for bcc and fcc crystal structures. Applying the umbrella sampling and adiabatic switching thermodynamic integration to spin-lattice dynamics simulations, we have evaluated the difference between the free energies of bcc and fcc phases as a function of temperature. Each free energy difference calculation referred to a particular temperature, hence avoiding the need to perform integration from 0 K, otherwise required in other simulation approaches (Lavrentiev et al. 2010).

Figure 3 shows the calculated free energy difference between the fcc and bcc phases. When the difference is positive, bcc phase is more stable, for example, at low temperatures. Otherwise, fcc phase is more stable. The curve crosses the horizontal axis at two points, near 1130 K and then again near 1600 K. These points correspond to the bcc-fcc $\alpha - \gamma$ and fcc-bcc $\gamma - \delta$ phase transitions, respectively. The predicted transition temperatures are close to the experimentally observed transition temperatures $T_{\alpha-\gamma} = 1185$ K and $T_{\gamma-\delta} = 1667$ K. The minimum free energy difference between the fcc and bcc phases is only -2 meV per atom. Analysis given in Lavrentiev et al. (2010) and Ma et al. (2017) shows that α-γ-δ phase transitions in magnetic iron stem from the interplay between magnetic excitations and lattice vibrations. The free energy contribution from non-collinear magnetic fluctuations reduces the free energy difference as temperature increases. When the temperature is higher than the Curie temperature T_C, the long-range magnetic order vanishes although the short-range order remains (see Ma et al. (2008) and Fig. 4).

At temperatures exceeding the Curie temperature, the contribution to entropy from magnetic excitations is superseded by the contribution from lattice vibrations, and it is the balance between entropy contributions to the free energy from spin and lattice dynamics that is ultimately responsible for the occurrence of the two, α-γ and γ-δ, rather than one, phase transitions in iron. This also illustrates the significance of taking into account spin-lattice coupling when modelling magnetic phase transitions in any real material.

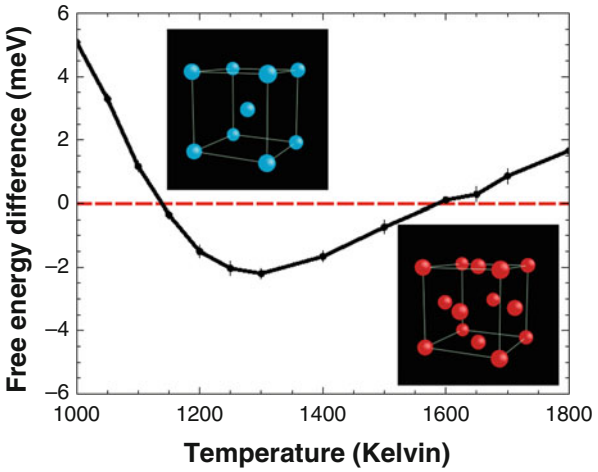

Fig. 3 Difference between the free energies of fcc and bcc phases of magnetic iron plotted as a function of temperature. Calculations were performed using a spin-lattice potential, taken as a sum of a nonmagnetic EAM potential and a Heisenberg-Landau Hamiltonian, as detailed by Eq. (27). The minimum free energy difference between fcc and bcc phases is −2 meV per atom

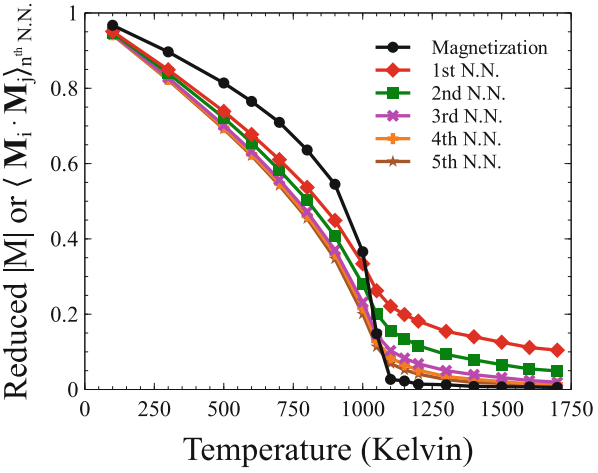

Fig. 4 Time average projection of an atomic spin on a magnetization axis and spin-spin short-range correlation functions evaluated for the first, second, . . ., fifth nearest-neighbor atoms and plotted as functions of absolute temperature. Long-range magnetic order vanishes at the Curie temperature T_C, whereas the magnetic short-range order does not vanish even at temperatures well above T_C

7 Outlook and Challenges

Applications of spin-lattice dynamics are still fairly sparse. The main difficulty associated with applications of spin-lattice dynamics is that, like molecular dynamics, spin-lattice dynamics requires a sufficiently accurate many-body spin-dependent potential. Although spin-lattice dynamics has been applied extensively to simulations of various microscopic dynamic effects in pure iron, including vacancy migration (Wen et al. 2013), and magnetic excitations in cobalt (Beaujouan et al. 2012), there is still no spin-lattice potential suitable for simulating mechanical deformations, magnetic fluctuations, and defect properties at the same time. There are two main reasons why this question remains outstanding.

First, the number of degrees of freedom in spin-lattice dynamics is twice that of molecular dynamics. In molecular dynamics, one needs to fit an interatomic interaction potential to input data based on atomic configurations in $3N$ dimensions, where N is the number of atoms in a simulation cell. In the case of spin-lattice dynamics, the number of degrees of freedom is $6N$ because each atom is characterized by its position as well as by the orientation and magnitude of the atomic magnetic moment. This poses a major challenge in the context of the fitting procedure as well as data generation and selection, since a significantly greater amount of data is required to span the multidimensional coordinate and spin phase space.

On the other hand, pure spin dynamics on a static lattice, which is a subset of spin-lattice dynamics, can be run as efficiently as MD. If we assume that the exchange coupling parameters J_{ij} are independent of atomic coordinates, the spin-dynamics part of the integration algorithm can be used for generating detailed information about magnetic phase transitions, as illustrated in Figs. 4 and 5.

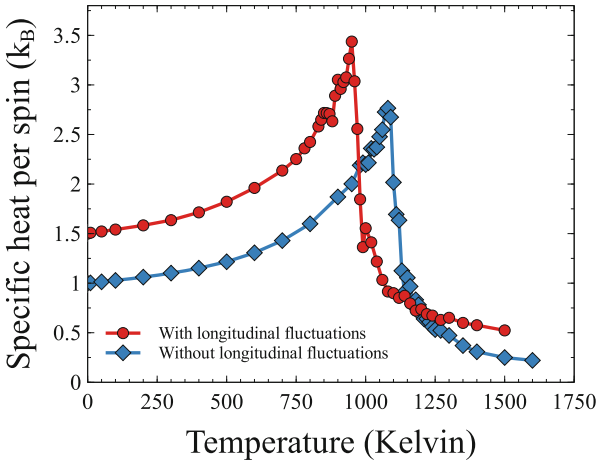

Fig. 5 Specific heat of bcc iron evaluated using purely rotational spin dynamics with no longitudinal fluctuations included, and Langevin spin dynamics taking longitudinal fluctuations of magnetic moments into account (Ma and Dudarev 2012). The peaks correspond to second-order magnetic phase transitions, where the long-range ferromagnetic order vanishes

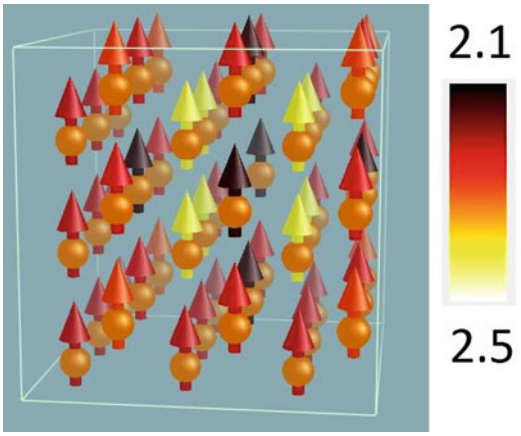

Fig. 6 Magnetic configuration of atoms in the vicinity of a mono-vacancy in ferromagnetic bcc iron, derived from ab initio calculations. The simulation cell contains 53 atoms. The magnitude of magnetic moments is greater in the first nearest-neighbor coordination shell of the vacancy, whereas magnetic moments are suppressed in the second nearest-neighbor coordination shell. Color refers to the magnitude of magnetic moments given by the scale bar, expressed in the Bohr magneton units

Second, a suitable functional form of the spin-lattice potential is yet to be firmly established. For example, if we adopt the form given by Eq. (27), we still do not know what functional form should be used for $J_{ij}(\mathbf{R})$, $A_i(\mathbf{R})$, and $B_i(\mathbf{R})$. In Figs. 6 and 7, we show a vacancy and a $\langle 110 \rangle$ self-interstitial dumbbell configurations in bcc ferromagnetic iron. These configurations were derived from ab initio calculations. We see that the magnitude and direction of magnetic moments depend on the local environment. Atoms near a defect have significantly different magnetic moments in comparison with moments of atoms in a perfect crystal. An often used pairwise form for $J_{ij}(\mathbf{R})$ does not fit the data for defects well, although it does fit reasonably well the data on magnetic moments in a nearly perfect lattice. A good spin-lattice potential should help model magnetic configurations associated with extended defects, such as line dislocations, dislocation loops, vacancy clusters, and voids, where ab initio calculations are still impossible or too computationally demanding.

In addition to defects, alloys present an even more challenging issue. Figure 8 shows the magnetic configuration of a FeCrNi ternary alloy. The data for the figure were taken from Wróbel et al. (2015). Even though the alloy adopts a nearly perfect fcc crystal structure, its magnetic configuration is fairly complex. This implies that a spin-lattice potential must contain information about the underlying spin-dependent electronic structure to be able to reproduce magnetic properties at a reasonable level of accuracy.

The functional form of a spin-lattice potential should reflect the many-body electron interactions. A recently derived tight-binding Hamiltonian (Coury et al. 2016) for non-collinear magnetic configurations is expected to provide a good starting point for a comprehensive treatment of this problem.

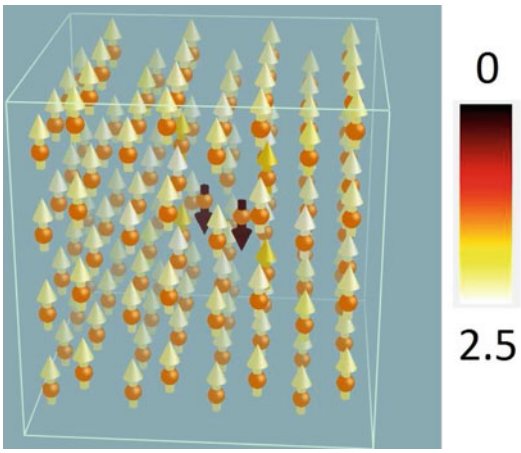

Fig. 7 A ⟨110⟩ self-interstitial dumbbell configuration in ferromagnetic bcc iron, predicted by ab initio calculations. The supercell contains 129 iron atoms. The magnitude of magnetic moments of the two atoms forming the center of the dumbbell is significantly smaller than that of the neighboring atoms. Magnetic moments of atoms in the center of the dumbbell have antiferromagnetic orientation with respect to the ferromagnetically ordered neighboring atoms. Color represents the magnitude of an atomic magnetic moment, expressed in the Bohr magneton units

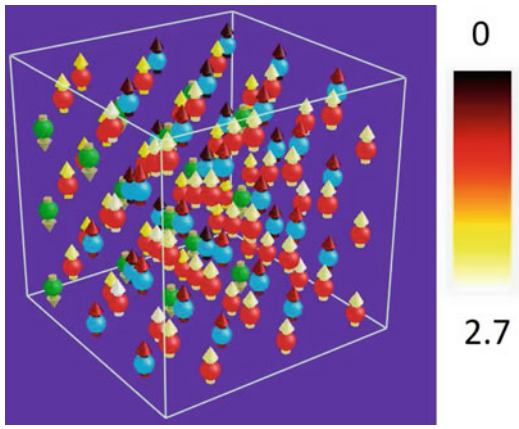

Fig. 8 Magnetic configuration of a FeCrNi fcc alloy containing 108 atoms in the simulation cell. The alloy configuration consists of 58 Fe atoms (red), 16 Cr atoms (green), and 34 Ni atoms (blue). Color of arrows refers to the magnitude of atomic magnetic moments defined by the scale bar, expressed in the Bohr magneton units

8 Conclusion

Spin-lattice dynamics is a powerful simulation tool for studying magnetic materials on the atomic scale. In this chapter, we have outlined the fundamental theory of spin-lattice dynamics and algorithms suitable for its numerical implementation.

Although there are still significant challenging issues that remain to be resolved, the field is open for exploration. Spin-lattice dynamics can be applied to a broad range of topics from modelling high-frequency electronic and magnetic devices to mechanical properties of magnetic alloys.

Acknowledgments This work has been carried out within the framework of the EUROfusion Consortium and has received funding from the Euratom research and training programme 2014–2018 under grant agreement No 633053 and from the RCUK Energy Programme (grant number EP/P012450/1). To obtain further information on the data and models underlying this paper, please contact PublicationsManager@ukaea.uk. The views and opinions expressed herein do not necessarily reflect those of the European Commission. We would like to thank Duc Nguyen-Manh for providing the data for Fig. 8.

References

Beaujouan D, Thibaudeau P, Barreteau C (2012) Anisotropic magnetic molecular dynamics of cobalt nanowires. Phys Rev B 86:174409. https://link.aps.org/doi/10.1103/PhysRevB.86.174409

Brown Jr WF (1963) Thermal fluctuations of a single-domain particle. Phys Rev 130:1677–1686. https://link.aps.org/doi/10.1103/PhysRev.130.1677

Chandrasekhar S (1943) Stochastic problems in physics and astronomy. Rev Mod Phys 15:1–89. https://link.aps.org/doi/10.1103/RevModPhys.15.1

Coury MEA, Dudarev SL, Foulkes WMC, Horsfield AP, Ma PW, Spencer JS (2016) Hubbard-like Hamiltonians for interacting electrons in s, p, and d orbitals. Phys Rev B 93:075101. https://link.aps.org/doi/10.1103/PhysRevB.93.075101

Daw MS, Baskes MI (1984) Embedded-atom method: derivation and application to impurities, surfaces, and other defects in metals. Phys Rev B 29:6443–6453. https://link.aps.org/doi/10.1103/PhysRevB.29.6443

Derlet PM, Nguyen-Manh D, Dudarev SL (2007) Multiscale modeling of crowdion and vacancy defects in body-centered-cubic transition metals. Phys Rev B 76:054107. https://link.aps.org/doi/10.1103/PhysRevB.76.054107

Dudarev SL, Derlet PM (2007) Interatomic potentials for materials with interacting electrons. J Computer-Aided Mater Des 14(Suppl 1):129–140. https://doi.org/10.1007/s10820-007-9073-x, https://link.springer.com/article/10.1007/s10820-007-9073-x

Finnis MW (2003) Interatomic forces in condensed matter. Oxford series on materials modelling. Oxford University Press, Oxford

Fu CC, Willaime F, Ordejon P (2004) Stability and mobility of mono- and di-interstitials in α-Fe. Phys Rev Lett 92:175503. https://link.aps.org/doi/10.1103/PhysRevLett.92.175503

Gilbert TL (2004) A phenomenological theory of damping in ferromagnetic materials. IEEE Trans Magn 40(6):3443–3449. https://doi.org/10.1109/TMAG.2004.836740

Hatano N, Suzuki M (2005) Finding exponential product formulas of higher orders. Springer, Berlin/Heidelberg, pp 37–68. https://doi.org/10.1007/11526216_2

Kubo R (1966) The fluctuation-dissipation theorem. Rep Prog Phys 29(1):255 http://stacks.iop.org/0034-4885/29/i=1/a=306

Landau LD, Lifshitz EM (1935) On the theory of the dispersion of magnetic permeability in ferromagnetic bodies. Phys Z Sowjetunion 8:153–164

Lavrentiev MY, Nguyen-Manh D, Dudarev SL (2010) Magnetic cluster expansion model for bcc-fcc transitions in Fe and Fe-Cr alloys. Phys Rev B 81:184202. https://link.aps.org/doi/10.1103/PhysRevB.81.184202

Lavrentiev MY, Soulairol R, Fu CC, Nguyen-Manh D, Dudarev SL (2011) Noncollinear magnetism at interfaces in iron-chromium alloys: the ground states and finite-temperature configurations. Phys Rev B 84:144203. https://link.aps.org/doi/10.1103/PhysRevB.84.144203

Ma PW, Woo CH (2009) Parallel algorithm for spin and spin-lattice dynamics simulations. Phys Rev E 79:046703. https://link.aps.org/doi/10.1103/PhysRevE.79.046703

Ma PW, Dudarev SL (2011) Langevin spin dynamics. Phys Rev B 83:134418. https://link.aps.org/doi/10.1103/PhysRevB.83.134418

Ma PW, Dudarev SL (2012) Longitudinal magnetic fluctuations in Langevin spin dynamics. Phys Rev B 86:054416. https://link.aps.org/doi/10.1103/PhysRevB.86.054416

Ma PW, Woo CH, Dudarev SL (2008) Large-scale simulation of the spin-lattice dynamics in ferromagnetic iron. Phys Rev B 78:024434. https://link.aps.org/doi/10.1103/PhysRevB.78.024434

Ma PW, Dudarev SL, Semenov AA, Woo CH (2010) Temperature for a dynamic spin ensemble. Phys Rev E 82:031111. https://link.aps.org/doi/10.1103/PhysRevE.82.031111

Ma PW, Dudarev SL, Woo CH (2012) Spin-lattice-electron dynamics simulations of magnetic materials. Phys Rev B 85:184301. https://link.aps.org/doi/10.1103/PhysRevB.85.184301

Ma PW, Dudarev SL, Woo CH (2016) SPILADY: a parallel CPU and GPU code for spin-lattice magnetic molecular dynamics simulations. Comput Phys Commun 207(Supplement C):350–361. https://doi.org/10.1016/j.cpc.2016.05.017, http://www.sciencedirect.com/science/article/pii/S0010465516301412

Ma PW, Dudarev SL, Wróbel JS (2017) Dynamic simulation of structural phase transitions in magnetic iron. Phys Rev B 96:094418. https://link.aps.org/doi/10.1103/PhysRevB.96.094418

Nguyen-Manh D, Horsfield AP, Dudarev SL (2006) Self-interstitial atom defects in bcc transition metals: group-specific trends. Phys Rev B 73:020101. https://link.aps.org/doi/10.1103/PhysRevB.73.020101

Omelyan IP, Mryglod IM, Folk R (2001a) Algorithm for molecular dynamics simulations of spin liquids. Phys Rev Lett 86:898–901. https://link.aps.org/doi/10.1103/PhysRevLett.86.898

Omelyan IP, Mryglod IM, Folk R (2001b) Molecular dynamics simulations of spin and pure liquids with preservation of all the conservation laws. Phys Rev E 64:016105. https://link.aps.org/doi/10.1103/PhysRevE.64.016105

Omelyan IP, Mryglod IM, Folk R (2002) Construction of high-order force-gradient algorithms for integration of motion in classical and quantum systems. Phys Rev E 66:026701. https://link.aps.org/doi/10.1103/PhysRevE.66.026701

Perera D, Eisenbach M, Nicholson DM, Stocks GM, Landau DP (2016) Reinventing atomistic magnetic simulations with spin-orbit coupling. Phys Rev B 93:060402. https://link.aps.org/doi/10.1103/PhysRevB.93.060402

Pettifor DG (1995) Bonding and structure of molecules and solids. Oxford science publications, Clarendon Press. https://books.google.co.uk/books?id=r7XGPHD24fgC

Tsai SH, Krech M, Landau DP (2004) Symplectic integration methods in molecular and spin dynamics simulations. Braz J Phys 34:384–391. http://www.scielo.br/scielo.php?script=sci_arttext&pid=S0103-97332004000300009&nrm=iso

Tsai SH, Lee HK, Landau DP (2005) Molecular and spin dynamics simulations using modern integration methods. Am J Phys 73(7):615–624. http://doi.org/10.1119/1.1900096

Van Kampen N (2011) Stochastic processes in physics and chemistry. North-Holland Personal Library, Elsevier Science. https://books.google.co.uk/books?id=N6II-6HlPxEC

Wen H, Ma PW, Woo C (2013) Spin-lattice dynamics study of vacancy formation and migration in ferromagnetic bcc iron. J Nucl Mater 440(1):428–434. https://doi.org/10.1016/j.jnucmat.2013.05.054, http://www.sciencedirect.com/science/article/pii/S0022311513008003

Wróbel JS, Nguyen-Manh D, Lavrentiev MY, Muzyk M, Dudarev SL (2015) Phase stability of ternary fcc and bcc Fe-Cr_{Ni} alloys. Phys Rev B 91:024108. https://link.aps.org/doi/10.1103/PhysRevB.91.024108

Zwanzig R (2001) Nonequilibrium statistical mechanics. Oxford University Press. https://books.google.co.uk/books?id=4cI5136OdoMC